# Hyperspectral Medical Images Unmixing for Cancer Screening Based on Rotational Independent Component Analysis

Bo Du[1], Nan Wang[2], Liangpei Zhang[2], and Dacheng Tao[3]

[1] School of Computer, Wuhan University
[2] LIESMARS, Wuhan University
[3] Centre for Quantum Computation and Intelligent Systems
University of Technology , Sydney
gunspace@163.com

**Abstract.** Hyperspectral images have shown promising performance in many applications, especially extracting information from remotely sensed geometric images. One obvious advantage is its good ability to reflect the physical meaning from a point view of spectrum, since even two very similar materials would present an obvious difference by a hyperspectral imaging system. Recent work has made great progress on the hyperspectral fluorescence imaging techniques, which makes the elaborate spectral observation of cancer areas possible. Cancer cells would be distinguishable with normal ones when the living body is injected with fluorescence, which helps organs inside the living body emit lights, and then the signals can be obtained by the passive imaging sensor. This paper discusses the ability to screen the cancers by means of hyperspectral bioluminescence images. A rotational independent component analysis method is proposed to solve the problem. Experiments evaluate the superior performance of the proposed ICA-based method to other blind source separation methods: 1) The ICA-based methods do perform well in detect the cancer areas inside the living body; 2) The proposed method presents more accurate cancer areas than other state-of-the-art algorithms.

**Keywords:** Cancer detection, hyperspectral images, independent component analysis.

## 1    Introduction

Much efforts have been done to combine the advantages of bioluminescence and fluorescence imaging [1, 2]. Actually, multispectral in vivo optical imaging technologies with bioluminescence and fluorescence is drawing great interest in recent years [3, 4, 5]. It employs bioluminescence and fluorescence imaging to obtain useful signals of receptors and has become another important biomedicine imaging techniques. Compared with the conventional biomedicine imaging techniques, such as ultrasonic, Computed tomography, Magnetic Resonance Imaging, positron emission tomography, it provides more straightforward measurements, much safer performance

and lower costs. One significant progress is the Maestro imaging system [6-8], which can obtain the hyperspectral images, covering the visible to near infrared with fine spectral resolution.

As to the hyperspectral image, it is a powerful way to describe the physical meaning of different materials [9]. Its foremost advantage is that the spectral resolution is very fine and the corresponding spectrum of each different material is continuous and smooth, showing diagonal features for elaborately separating visually very similar objects. So hyperspectral images provides a new way to analyze the distribution of materials of interest [10], which have been widely used in geometrical information extraction. Classical methods employ the spectral unmixing to do the task. It is assumed that the pixels in the image are linear composed of limited materials' spectra (called endmembers) and the corresponding abundances. This is the so called linear mixture model (LMM) [11, 12, 13]. There are two ways for spectral unmixing: getting the typical spectra for each material and then the abundances can be obtained by least squares methods with these spectra; unmixing the pixels into the spectra and the abundances simultaneously [14, 15, 16]. The latter approach is usually achieved by blind source separation based methods, including independent component analysis and nonnegative matrix fraction methods [17-23]. But, these ICA-based methods cannot obtain nonnegative abundances which is necessary in explaining the objects' distributions and NMF are susceptible to the initial values.

This paper aims to address the cancer screening problem from a hyperspectral fluorescence images. A rotational independent component analysis is developed to hyperspectral unmxing. The rotational ICA rotates the coordinate system of the dataset with a serial of orthogonal rotation matrix until all the data fall in the first quadrant. Compared with traditional ICA, the result of the rotational ICA can make most abundances values non-negative, satisfying the abundance non-negative constraint, which is an important property in reality. With the accurate abundance vectors, reliable endmembers can also be obtained. Besides, the proposed rotational ICA can be achieved without a proper initialization.

The remainder of this paper is organized as follows. Section 2 presents the LMM and basic ICA model. Section 3 details the rotational ICA method and applies it to hyperspectral unmxing. The experiments on the fluorescence dataset are described in Sections 4, respectively. Section V concludes the paper.

## 2    Spectral Unmixing Model in Hyperspectral Images

### 2.1    A Linear Mixture Model (LMM)

The LMM assumes that one pixel in the hyperspectral dataset is a linear mixture of $P$ known material signatures, called endmembers: $A = [a_1, a_2, ..., a_P]$, where $a_i$ is one of the endmember spectra with dimension "$band$". The corresponding proportion is called the abundance: $S = [s_1^T, s_2^T, ..., s_P^T] = [\omega_1, \omega_2, ..., \omega_N]$, where each column $s_i^T$ is a $N$-dimension vector, corresponding to the $ith$ spectra in $A$. Based on LMM, each pixel in a hyperspectral image dataset can be expressed as :

$$x = A\omega + \varepsilon \tag{1}$$

where $x$ is a $band \times 1$ vector representing one pixel in the hyperspectral image, and $\varepsilon$ is the residual error. According to LMM, the abundance matrix should satisfy the ASC and abundance non-negative constraints (ANC) simultaneously, i.e., $s_1^T + s_2^T + ... + s_p^T = \mathbf{1}^T$ and $s_i^T \geq 0$

## 3    Rotational ICA for Hyperspectral Bioluminescence Images

In the traditional ICA, whitening is an important step before ICA iteration procedure [11]. Because it can achieve the half-work of the ICA, removing any second-order dependencies in the dataset. The whitened dataset always exists negative values (Figure 1). In order to make the whitened datase t fall in the first quadrant, which leads the results non-negative, the rotation is needed.
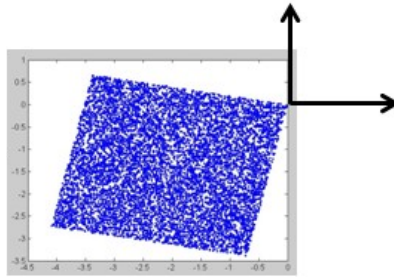


**Fig. 1.** The whitened dataset in two dimensions

The rotation matrix can be defined as:

$$W = \begin{pmatrix} \cos\phi & \sin\phi \\ -\sin\phi & \cos\phi \end{pmatrix} \tag{2}$$

Through the rotation matrix, the coordinate system will be anticlockwise rotated and then some points will fall in the first quadrant. The matrix $W$ is determined by the rotation angle $\phi$ and with the formula (4) $W$ is constrained to be orthogonal. The new coordinate values with the rotation matrix $W$ can be obtained as:

$$\begin{cases} y_1 = x_1 \cos\phi + x_2 \sin\phi \\ y_2 = x_2 \cos\phi - x_1 \sin\phi \end{cases} \tag{5}$$

To find the rotation matrix $W$, an objective function in 2-dimensions case is defined as:

$$\min_{J} \; J = \begin{cases} 0 & if \quad y_1 \geq 0 \;\; and \;\; y_2 \geq 0 \\ y_2^2 & if \quad y_1 \geq 0 \;\; and \;\; y_2 < 0 \\ y_1^2 & if \quad y_1 < 0 \;\; and \;\; y_2 \geq 0 \\ y_1^2 + y_2^2 & otherwise \end{cases} \qquad (6)$$

where the function value is equal to zero when the point falls in the first quadrant, otherwise, equal to non-zero. Differentiating (6) with respect to the rotation angle $\phi$, we get:

$$-\frac{\partial J}{\partial \phi} = \begin{cases} 0 & if \quad y_1 \geq 0 \;\; and \;\; y_2 \geq 0 \\ y_2 y_1 & if \quad y_1 \geq 0 \;\; and \;\; y_2 < 0 \\ -y_1 y_2 & if \quad y_1 < 0 \;\; and \;\; y_2 \geq 0 \\ 0 & otherwise \end{cases} \qquad (7)$$

We can minimize the problem (6) by finding a zero of the equation (7) with respect to the rotation angle $\phi$. There are many standard methods available to find the zero of a function, a *fzero* in the Matlab function can be used to find the zero of the equation (7).

For n-dimension case, a general n-dimensional orthogonal transform can be formed from a product of 2-D rotations. In the iteration procedure, calculate the values of equation (7) for each axis pair and rotate the axis pair with the highest value.

Based on LMM, hyperspectral unmxing can be considered as a problem that extracts potential components from the observations. Consider the abundance vectors as independent components, we can perform hyperspectral unmxing based on rotational ICA. Because the abundance vectors are correlative each other, we whiten the orignal dataset with correlation matrix, not the covariance matrix, to keep the dataset correlative. The whole algorithm is as follows:

1) Whiten the original dataset $X$. Calculate the correlation matrix of original dataset:

$$\sum = XX^T / N \qquad (8)$$

where $N$ is the number of pixels. Calculate the eigenvalues matrix $D$ and eigenvectores matrix $E$ of the $\sum$, and reduce the dimension of original dataset to $p$-dimensions with

$$Z = (D_p^{-1/2} E_p^T) X \qquad (9)$$

where $D_p$ is a diagonal matrix with the first $p$ eigenvalues in the diagonal line $E_p$ is the corresponding vectors. Set $Z(0) = Z$ and $W(0) = I_n$ for $t = 0$.

2) Calculate the output abundances $Y = Z(t) = W(t)Z(0)$ and set $Y_+$ with $y_{ik}^+ = \max(y_{ik}, 0)$ and $Y_-$ with $y_{ik}^- = \min(y_{ik}, 0)$

3) Calculate the values of equation (7) for all axis pairs

$$g_{ij} = \sum_k y_{ik}^+ y_{jk}^- - y_{ik}^- y_{jk}^+$$

4) If the maximum value of $\left| g_{ij} \right|$ is less than the tolerance required, stop. Otherwise, continue the following step.

5) Choose the axis pair $i^*, j^*$ with max value in $\left| g_{ij} \right|$ and select rows $i^*, j^*$ from matrix $Z(t)$ to construct the $2 \times p$ matrix $Z^*$

6) Using the reduced data $Z^*$ to minimize the problem (6). Search a rotational angle $\phi$ to make the value of formula (7) be zero. This rotation angle is the stationary point of the function (6) which lead the exterma of the function (6).

7) Calculate the rotation matrix $R(t+1) = [r(t+1)_{ij}]$ with $\phi^*(t+1)$, where $r_{i^*i^*} = r_{j^*j^*} = \cos(\phi^*)$ , $r_{j^*i^*} = -\sin(\phi^*)$ , $r_{i^*j^*} = \sin(\phi^*)$ , $r_{ii} = 1$ for all $i \neq i^*, j^*$ and all other entries of R are zero.

8) Set $W(t+1) = R(t+1)W(t)$ and $Z(t+1) = R(t+1)Z(t)$

9) Set $t = t+1$ and go to step (2) until the max value of $\left| g_{ij} \right|$ is close to zero.

10) Repeating the step (2)-(9) in the procedure of non-negative ICA and get the abundance matrix $S$. According to $X$ and $S$ in the linear mixture model, calculate the endmember matrix $A$ with the least squares estimation.

## 4     Experiments

In the experiment, three methods — FAST_ICA[11]、SISAL[9] and CICA[23] are employed to evaluate the efficient of the proposed strategy. The simplex identification via split augmented Lagrangian (SISAL) algorithm, which enforced the endmembers' spectral vectors to compose a convex hull containing all the pixels in the image, constrained by soft constraints. We use SISAL to extract the endmember signatures and calculate the abundance with least square algorithm.

The spectral angle distance (SAD) [2] is used to evaluate the accuracy of the extracted endmember signatures. The SAD values of the algorithms are showed in

Table 1 and the abundance maps are plotted in Figure 2. It is revealed that our proposed method presents the best endmembers, with the least SAD values for cancer areas and the other areas. From the abundance maps, it is also obvious that the cancer distribution is more accurate in our method.
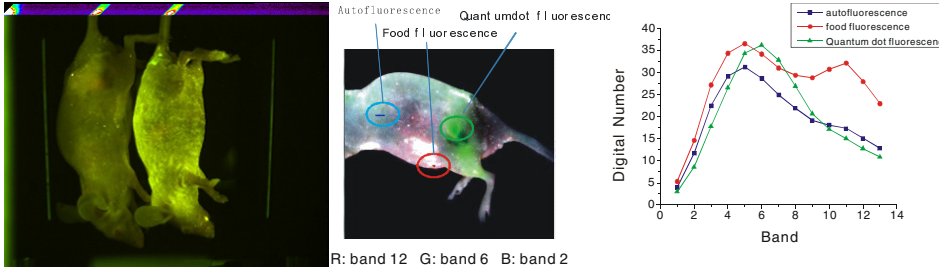


Hyperspectral Bioluminescence Datacube

The false color picture of the datacube in our experiments and the most concentrated areas for each fluorescence material

The reference spectra of three materials

**Table 1.** SAD values for different algorithm

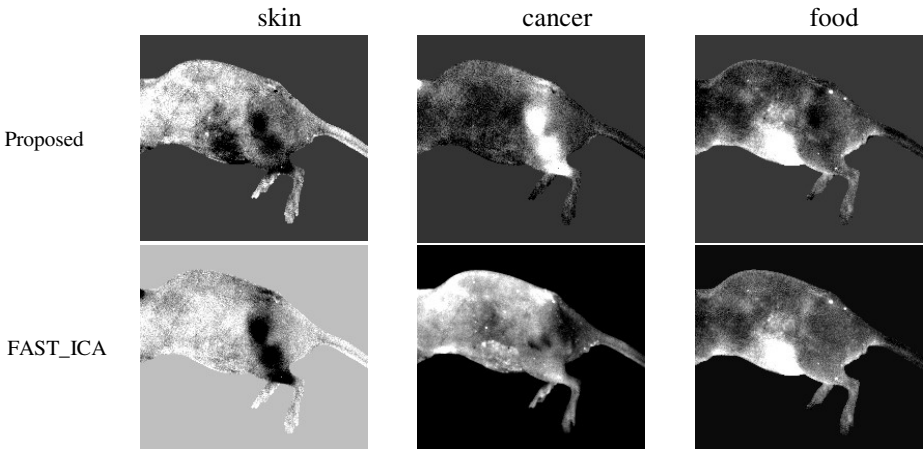|  | skin | cancer | food | average |
|---|---|---|---|---|
| Proposed | **0.2048** | **0.0722** | 0.0282 | **0.1018** |
| FAST_ICA | 1.1062 | 0.0634 | 0.2342 | 0.4679 |
| SISAL | 2.8786 | 0.1211 | 0.0832 | 1.0277 |
| CICA | 0.2051 | 0.0815 | **0.0258** | 0.1041 |



**Fig. 2.** The abundance maps of different algorithms

**Fig. 2.** (*Continued.*)

## 5    Conclusion

This paper proposes a rational based ICA, focusing on solving the cancer screening problem from hyperspectral medical images. By a rational transformation, most of the abundances values can be nonnegative and the corresponding spectra are also accurate . Experimental results show its superior performance than conventional methods.

## References

[1] Wang, X., Rosol, M., Ge, S., et al.: Dynamic tracking of human hematopoietic stem cell engraftment using in vivo bioluminescence imaging. Blood 102, 3478–3482 (2003)
[2] Levenson, R.M., Lynch, D.T., Kobayashi, H., et al.: Multiplexing with Multispectral Imaging: From Mice to Microscopy. ILAR Journal 49(1), 78–88 (2008)
[3] Zhang, Y., Han, Y., Zhao, C.L., et al.: Current developments in animal in vivo optical imaging technologies with bioluminescence and fluorescence. Chinese Bull. Life Sci. 18(1), 25–30 (2006)
[4] Mansfield, J.R., Hoyt, C., Levenson, R.M.: Visualization of Microscopy-Based Spectral Imaging Data from Multi-Label Tissue Sections. Current Protocols in Molecular Biology 14(19), 1–14 (2008)
[5] Ntziachristos, V., Ripoll, J., Wang, L.V., et al.: Looking and listening to light the evolution of whole - body photonic imaging. Nat. Biotechnol. 23(3), 313–320 (2005)
[6] Harris, S., Wallace, R.: Acousto-optic tunable filter. Journal of the Optical Society of America 59, 744–747 (1969)

[7]  Gebhart, S.C., Thompson, R.C., Mahadevan-Jansen, A.: Liquid-crystal tunable filter spectral imaging for brain tumor demarcation. Applied Optics 46, 1896–1910 (2007)

[8]  Cai, W., Chen, X.: Preparation of peptide-conjugated quantum dots for tumor vasculature-targeted imaging. Nature Protocols 3, 89–96 (2008)

[9]  Plaza, A., Martinez, P., Perez, R., Plaza, J.: Spatial/spectral endmember extraction by multidimensional morphological operations. IEEE Trans. Geosci. Remote Sens. 40(9), 2025–2041 (2002)

[10] Bioucas-Dias, J.M.: A variable splitting augmented Lagrangian approach to linear spectral unmixing. In: First Workshop on Hyperspectral Image and Signal Processing: Evolution in Remote Sensing, WHISPERS 2009, pp. 1–4 (2009)

[11] Hyvarinen, A., Karhunen, J., Oja, E.: Independent Component Analysis. Wiley, New York (2001)

[12] Lee, D.D., Seung, H.S.: Algorithms for non-negative matrix factorization. Adv. Neural Inf. Process. Syst. 13, 556–562 (2000)

[13] Donoho, D., Stodden, V.: When Does Non-Negative Matrix Factorization Give a Correct Decomposition Into Parts (2003)

[14] Zhou, G.X., Xie, S.L., Ding, S.X., Yang, J.M., Zhang, J.: Blind Spectral Unmixing Based on Sparse Nonnegative Matrix Factorization. IEEE Trans. Image Process. 20, 1112–1125 (2011)

[15] Huck, A., Guillaume, M., Blanc-Talon, J.: Minimum Dispersion Constrained Nonnegative Matrix Factorization to Unmix Hyperspectral Data. IEEE Trans. Geosci. Remote Sens. 48, 2590–2602 (2010)

[16] Miao, L., Qi, H.: Endmember extraction from highly mixed data using minimum volume constrained nonnegative matrix factorization. IEEE Trans. Geosci. Remote Sens. 45(3), 765–777 (2007)

[17] Jia, S., Qian, Y.T.: Constrained Nonnegative Matrix Factorization for Hyperspectral Unmixing. IEEE Trans. Geosci. Remote Sens. 47, 161–173 (2009)

[18] Liu, X.S., Xia, W., Wang, B., Zhang, L.M.: An Approach Based on Constrained Nonnegative Matrix Factorization to Unmix Hyperspectral Data. IEEE Trans. Geosci. Remote Sens. 49, 757–772 (2011)

[19] Bayliss, J., Gualtieri, J.A., Cromp, R.F.: Analyzing hyperspectral data with independent component analysis. In: Proc. SPIE, vol. 3240, pp. 133–143 (1997)

[20] Chen, C., Zhang, X.: Independent component analysis for remote sensing study. In: Proc. SPIE, vol. 3871, pp. 150–158 (1999)

[21] Moussaoui, S., Hauksdottir, H., Schmidt, F., Jutten, C., Chanussot, J., Brie, D., Doute, S., Benediktsson, J.A.: On the decomposition of Mars hyperspectral data by ICA and Bayesian positive source separation. Neurocomputing 71(10-12), 2194–2208 (2008)

[22] Nascimento, J., Bioucas-Dias, J.: Hyperspectral unmixing algorithm via dependent component analysis. In: Proc. IEEE IGARSS, pp. 4033–4036 (July 2007)

[23] Xia, W., Liu, X., Wang, B., Zhang, L.: Independent Component Analysis for Blind Unmixing of Hyperspectral Imagery with Additional Constraints. IEEE Transactions on Geoscience and Remote Sensing 49(6), 2165–2179 (2011)